



HAL
open science

Techno-economical modelling of a power-to-gas system for plant configuration evaluation in a local context

Corey Duncan, Robin Roche, Samir Jemei, Marie-Cécile Péra

► To cite this version:

Corey Duncan, Robin Roche, Samir Jemei, Marie-Cécile Péra. Techno-economical modelling of a power-to-gas system for plant configuration evaluation in a local context. *Applied Energy*, 2022, 315, pp.118930. hal-03692975

HAL Id: hal-03692975

<https://hal.science/hal-03692975>

Submitted on 10 Jun 2022

HAL is a multi-disciplinary open access archive for the deposit and dissemination of scientific research documents, whether they are published or not. The documents may come from teaching and research institutions in France or abroad, or from public or private research centers.

L'archive ouverte pluridisciplinaire **HAL**, est destinée au dépôt et à la diffusion de documents scientifiques de niveau recherche, publiés ou non, émanant des établissements d'enseignement et de recherche français ou étrangers, des laboratoires publics ou privés.

Highlights

Techno-economical modeling of a power-to-gas system for plant configuration evaluation in a local context

Corey Duncan, Robin Roche, Samir Jemei, Marie-Cecile Pera

- Holistic power-to-gas modeling methodology for project techno-economical analysis is presented.
- Scenarios based upon different configurations and electricity cost structures analysed for a pilot project in Europe.
- Best scenarios include synthetic natural gas grid injection and mobility.
- Minimum selling price found to be significantly higher than current natural gas prices.
- Sensitivity analysis shows electrolyser efficiency and electricity price most influential.

Techno-economical modeling of a power-to-gas system for plant configuration evaluation in a local context

Corey Duncan^{a,*}, Robin Roche^b, Samir Jemei^a, Marie-Cecile Pera^a

^a*FEMTO-ST Institute, FCLAB, Univ. Bourgogne Franche-Comté, CNRS, Belfort, France*

^b*FEMTO-ST Institute, FCLAB, Univ. Bourgogne Franche-Comté, UTBM, CNRS, Belfort, France*

Abstract

Decarbonization of the European energy networks is critical to meet Commission targets in the coming decades. The presented study aims to contribute to this by analysing one of the proposed solutions: power-to-gas. A techno-economic model is created for the purposes of evaluating specific projects on their feasibility in terms of local constraints and opportunities, using a current project as a template for model generation and analysing different possible configurations in 8 operational scenarios. Five metrics were used for scenario analysis: levelized cost of methane, minimum selling price, operational hours, hydrogen tank size and capital cost. The results from the analysis indicate that, in terms of the stated project, synthetic natural gas production and grid injection along with on-site mobility applications provide the best economical result. However, selling prices of synthetic natural gas obtained are one magnitude higher than current natural gas prices, in-

*Corresponding author

Email addresses: corey.duncan@univ-fcomte.fr (Corey Duncan),
robin.roche@femto-st.fr (Robin Roche), samir.jemei@femto-st.fr (Samir Jemei),
marie-cecile.pera@femto-st.fr (Marie-Cecile Pera)

dicating government support is required for further development. Future projections of electrolyser efficiency and equipment capital costs will greatly reduce production costs, giving promise for feasible business cases in the coming years.

Keywords: power-to-gas, system modeling, techno-economical analysis, synthetic natural gas

Nomenclature

Abbreviations

BOP balance of plant

CNG compressed natural gas

DA day-ahead

FCR frequency containment reserve

GHG greenhouse gas

LCOE levelized cost of energy

NG natural gas

OH operational hours

PEM polymer electrolyte membrane

PtG power-to-gas

PtX power-to-X

SNG synthetic natural gas

TSO transmission system operator

VRE variable renewable energy

WTP willingness to pay

Parameters

c_{BOP} cost of BOP (% of CAPEX)

$c_{var,rea}$ cost of reactor nutrient (€/Nm³)

$CAPEX$ total capital expenditure in year 0, including BOP (€)

$CAPEX_{equip}$ total capital expenditure in year 0 (€)

$cons_{grid,t}$ local NG grid consumption at time step t (Nm³/10min)

f_n nominal electrical grid frequency (Hz)

f_t electrical grid frequency at time step t (Hz)

K FCR gain (MW/Hz)

k_a discount factor

n project lifespan (years)

$OH_{x,max}$ maximum yearly operational hours for equipment x (hours)

$OPEX$ total yearly operational expenditure (€)

$OPEX_{fix}$ total yearly fixed operational expenditure (€)

$P_{elect,min}/P_{elect,max}$ electrolyser minimum/maximum power rating (MW)

$p_{min,tank}/p_{r,tank}$ minimum/rated tank pressure (bar)

$P_{r,elect}$ electrolyser rated power (MW)

$Q_{H_2,rea,min}/q_{H_2,rea,max}$ reactor minimum/maximum H₂ consumption (Nm³/10min)

$Q_{H_2,rea,t}$ reactor H₂ consumption at time step t (Nm³)

r discount rate (%)

rr_{rea} reactor ramping rate (Nm³/10min)

t current time step of simulation $\forall t \in m$

v_{FCR} price value of FCR participation (€/MW/h)

v_{H_2} price value of H₂ for mobility (€/kg)

WTP_{det} pre-determined willingness to pay (€/MWh)

Variables

C_{rep} total levelized cost of equipment replacement during the project lifespan (€)

F total yearly cost of feedstocks

$OPEX_{var}$ total yearly variable operational expenditure (€)

$P_{elect,tot,t}$ total electrolyser power at time step t , including FCR participation (MW)

$P_{elect,t}$ electrolyser power at time step t (MW)

$P_{FCR,t}$ electrolyser power adjustment when participating in the FCR (MW)

$p_{tank,t}$ tank pressure at time step t (bar)

$Q_{CNG,r}$ rated SNG production used for CNG mobility (Nm³)

$Q_{H_2,mob,t}$ H₂ production used for mobility at time step t (Nm³)

$Q_{H_2,mob}$ yearly H₂ production used for mobility (Nm³)

Q_{SNG} total yearly SNG production (Nm³)

R_{FCR} yearly revenue from FCR participation (€)

R_{H_2} yearly revenue from H₂ mobility (€)

$sig_{FCR,t}$ signal of electrolyser participation in the FCR at time step t

LCOM levelized cost of methane (€/MWh)

MSP minimum selling price (€/MWh)

1. Introduction

The 2030 Climate and Energy Framework (CEF) for the European Union (EU) has translated Paris Agreement commitments to mandatory EU-wide targets, specifically: reducing greenhouse gas (GHG) emissions by 40% from 1990 levels and increasing the share of renewables in primary energy to 32.5% [1]. Achieving the CEF targets as well as meeting higher demands of electrical energy are fueling a large up-take of variable renewable energy (VRE),

8 namely wind and solar. However, energy systems with high shares of VREs
9 require flexibility due to the spatial and temporal imbalances of supply and
10 demand, which can be provided by multiple approaches, each with unique
11 economical and technical benefits [2].

12 One such approach is using energy storage technologies as a means to
13 absorb surplus electricity, shifting its time of delivery for periods of greater
14 demand. Pumped hydro power is currently the primary energy storage tech-
15 nology used for electricity, with massive facilities worldwide. Several emerg-
16 ing storage solutions involve power-to-X (PtX) technologies, with over 150
17 demonstration projects in Europe either planned, operational or completed
18 [3]. PtX can be defined as electrical power conversion to other energy ap-
19 plications, such as: transportation fuels, heating, chemical feedstock to pro-
20 duce liquid fuels or other chemicals or re-converted to power. A diagram of
21 possible PtX pathways is shown in Figure 1. As is shown, PtX allows inte-
22 gration of gas and electricity networks, which provides several benefits such
23 as: further improving flexibility of the system to integrate VREs, short-
24 long-term energy storage capabilities [4] and helping to decarbonize sectors
25 other than electricity. [5]. When coupled with local VREs, it has been shown
26 to decrease curtailment and avoid additional electrical infrastructure costs by
27 using already available gas grid installations [6]. The main concept of PtX –
28 producing energy-rich gases such as hydrogen (H_2) and methane (CH_4) from
29 renewable energy sources – is called power-to-gas (PtG).

30 The core conversion of PtG pathways is water electrolysis: electrical dis-
31 sociation of water (H_2O) to H_2 and oxygen (O_2). The H_2 gas can be used
32 for transportation, providing significant sector carbon emission reduction po-

33 tential when compared to fossil fuels [7] as well as longer range and higher
34 specific energy (when compressed to 350 or 700 bar) than batteries [8]. It
35 can also be directly injected into the natural gas (NG) grid, with a volumet-
36 ric capacity of 0.1%-12% depending upon the respective European country's
37 standards [9]. PtG also includes the possibility of further processing H_2 by
38 combining it with carbon to produce methane (CH_4) via the Sabatier pro-
39 cess in methanation reactors. The most common H_2 conversion process done
40 in PtX projects [10], CH_4 reactors can be classified as either biological or
41 catalytic. Biological reactors produce CH_4 using organic matter, namely hy-
42 drogenotrophic methanogens, in a low pressure and temperature environment
43 [5] whereas catalytic reactors use nickel-based catalyst using high pressure
44 and temperature [11]. The choice of proper technology depends on the sys-
45 tem requirements, with biological reactors allowing higher levels of impurities
46 and catalytic reactors achieving higher production rates [5]. Carbon dioxide
47 (CO_2) is increasingly used as the carbon source for CH_4 production due to:
48 (1) high availability as a byproduct from industrial, waste treatment and
49 biogas facilities; (2) the reduction of CO_2 in the atmosphere; and (3) its low
50 cost of 0-100 €/ton [11]. The product CH_4 is also known as synthetic natural
51 gas (SNG) as it can be directly injected into the NG grid due to its similar
52 physical properties, allowing the over 1,000 TWh European NG network ca-
53 pacity to be used for transmission, distribution and storage of the product
54 gas [12]. In addition to the plethora of PtG production end-uses, it is also
55 viewed as a technology capable of providing electricity grid ancillary services,
56 ensuring grid stability in short (seconds) to long (months) durations [13].

57 Further development of the technologies involved in PtG as well as scaling

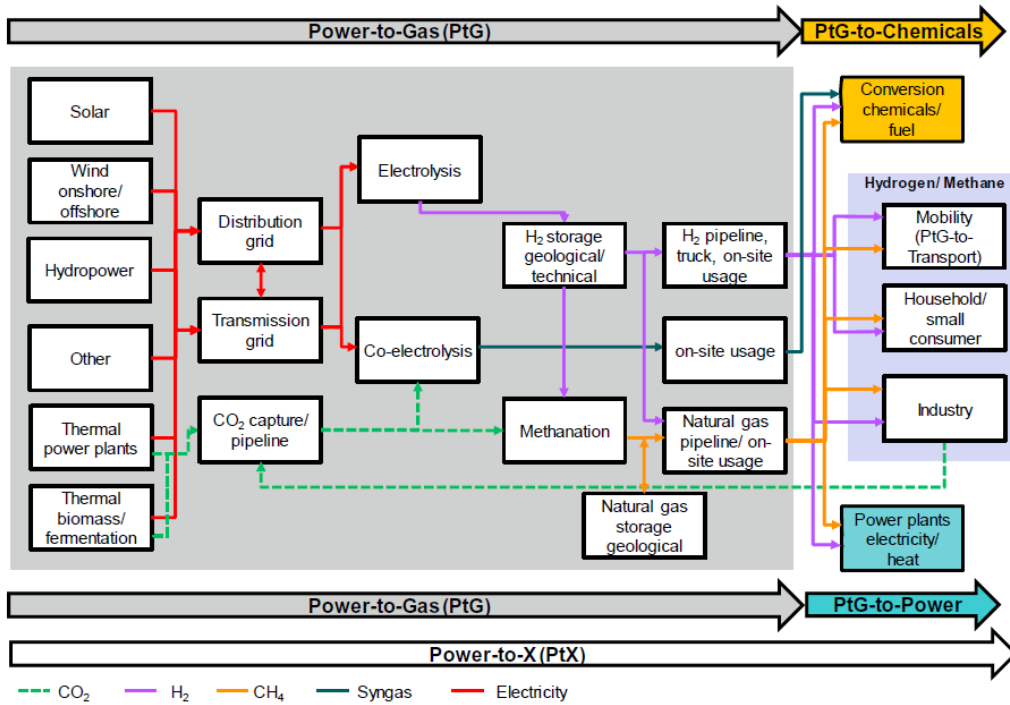


Figure 1: Overview of power-to-X pathways; source [14].

58 up are required to improve its economics. Götz et al. [11] and van Leeuwen
 59 and Zauner [15] concluded that high investment and electricity costs are the
 60 primary reasons for poor economics, with high yearly operational hours (OH)
 61 needed to reduce their effect. The inevitable high cost of the equipment can
 62 be attributed to the novelty of the technologies, namely (other than alka-
 63 line) electrolysis and methanation [16]. Nonetheless, PtG installed capacity
 64 has been exponentially increasing since the early 2000's as their costs con-
 65 tinue to fall and business cases become realized [3]. De Bucy et al. [17]
 66 assessed the economical potential of PtG in Europe, concluding that mo-
 67 bility is the best current market with high OH and low electricity prices.
 68 Further, they found that the levelized cost of H₂ and SNG for grid injec-

tion were 5 and 8.5 times the current selling price of NG, respectively, and SNG costs 1.5-3 times higher than bio-NG, highlighting the need for regulatory incentives for commercial deployment. McDonagh et al. [18] studied SNG production as a transport fuel, calculating a cost of 107-143 €/MWh in 2020 when assuming an average electricity price of 35 €/MWh and 6,500 OH. They also showed the impact of several incentives schemes that could help lower the cost below NG, such as selling produced O₂ and grid services. However, this study focuses on a national level (Ireland) and does not discuss cost reduction strategies for individual plants. Flexible plant operation has been found to be economically preferred – operating the system when electricity prices are favorable versus continuous operation – with more than one revenue stream harnessed. Breyer et al. [19] modeled a PtG plant used on-site of a pulp mill in Finland with frequency containment reserve (FCR) market participation and 4,000 OH and found the business case to be profitable, with grid services representing 40% of total income. Bio-diesel and SNG produced were either used on-site or sold for mobility purposes. However, this model used an assumed fixed electricity price of 40 €/MWh, neglecting actual dynamic day-ahead (DA) electricity market participation. Limitations on local gas consumption were also not considered. Tractebel and Hinicio [20] designed three business case opportunities in Europe using local conditions with mobility and industry seen as the best current primary applications. DA market participation was considered, with a yearly average price below 40-50 €/MWh required to build a profitable business case. FCR participation was also found to reduce payback time by 30-50%, signifying its importance to profitability. However, the study only considered H₂ as a

94 PtG product, neglecting the potential of SNG and other byproducts. Gorre
95 et al. [21] performed an optimization analysis of production costs of SNG in
96 terms of various electricity purchasing and gas selling strategies for a PtG
97 plant in 2030 and 2050, comparing them to the expected SNG prices. The
98 results showed that flexible operation in DA markets with an average price
99 of 30 €/MWh and 4,000 OH can have a positive revenue by 2050. However,
100 the study is generic to Europe and does not consider participation in ancil-
101 lary services, local technical or physical limitations, governmental support
102 schemes or specific country DA electricity prices. From this literature review
103 it is seen that most studies perform European-wide analyses suggesting broad
104 action without considering local limitations or advantages, such as regional
105 end-use applications, local restrictions in energy networks (namely NG and
106 electricity networks for purposes of this paper) and DA energy prices. These
107 parameters can and ultimately determine the viability of projects and allow
108 a thorough investigation of local business case opportunities.

109 The scientific contribution of this paper is to present a methodology for
110 performing a feasibility study of a PtG plant which focuses on analysing local
111 conditions which effect operation, namely: variable electrical power source,
112 DA variable and fixed electricity prices, possible local end-use applications
113 and local gas grid injection limitations. Individually, these parameters can
114 have profound implications on operational strategy; together they can com-
115 pletely change the plant's operational objective and its feasibility by giving a
116 more complete picture of it's unique conditions. This methodology is applied
117 to a pilot project currently underway in the form of a case study. Although
118 the specific model created for this case study cannot be used for other projects

119 as they all will have unique local conditions, it is believed that the methodol-
120 ogy presented can be easily applied to similar projects, providing a thorough
121 analysis of project feasibility. Further, an innovative electrolyser design is
122 investigated that allows maximum capacity to be 200% rated for short dura-
123 tions. This can allow participation in ancillary services while not sacrificing
124 on lost production due to reserved power or over-sizing the electrolyser for
125 such service. As previously mentioned, high investment and electricity costs
126 will present a major challenge in finding an optimal operational configuration
127 that is profitable. To overcome this challenge, an analysis of the most influ-
128 ential economical factors will be done, highlighting what needs to be done to
129 make a similar project feasible.

130 The objectives of this paper are to:

- 131 • Present a techno-economical model methodology for PtG plant analysis
132 using local limitations and opportunities as operating constraints and
133 several metrics for thorough analysis.
- 134 • Present the pilot project that will be used as a case study of model
135 methodology application.
- 136 • Develop operational scenarios based off of local conditions for the pilot
137 project and perform a feasibility study.
- 138 • Perform a sensitivity analysis on the most favorable scenarios to deter-
139 mine most influential factors on the results.

140 **2. Methodology**

141 *2.1. Standard Configuration of Pilot Plant*

142 To develop the model, a current PtG project in which the authors are
143 involved in named HYCAUNAIS is used. Located in Saint-Florentin, France
144 the project is being led by Storengy and has several industrial and public
145 partners, with secured funding from PIA ADEME, Bourgogne France-Comté
146 region (FRI), FEDER and project partners [22]. As the project is based in
147 France, regulatory and market conditions there will be used henceforth. It
148 must be emphasized that the work performed for this paper is researched-
149 based and not representative of actual project objectives of HYCAUNAIS -
150 it is meant to analyse several possible scenarios which are based upon the
151 project topology.

152 A diagram of the HYCAUNAIS plant layout and possible configurations
153 is shown in Figure 2. The plant will produce low-carbon gas for NG grid
154 injection and possibly mobility. Following the combined power production
155 signal of two existing wind farms (1) provided by the wind farm operator and
156 sourcing the electricity via a grid connection (2), a 1 MW_{el} PEM electrolyser
157 (3) will produce hydrogen for a 50 Nm³/h biological methanation reactor
158 (4), with intermediate H₂ storage (5) installed between the electrolyser and
159 reactor. Currently, gas from the landfill (6) on-site is being upgraded by
160 a WAGABOX[®] unit (7). The technology, supplied by Waga Energy [23],
161 combines membrane filtration and cryogenic distillation to filter 98 vol%
162 pure bio-CH₄ from landfill gas (CH₄ from a landfill is considered biological
163 as per French regulation [24] and international agencies such as the IEA [25]),
164 recovering 90 vol% of the bio-CH₄ contained in it. This highly pure bio-CH₄

165 is being injected into the NG grid (8). The CO₂ stream (including some
 166 impurities) normally vented during membrane distillation will be utilized as
 167 the carbon source for methanation, which must be purified (9) prior to in-
 168 jection into the biological reactor. Intermediate storage of CO₂ (10) between
 169 the reactor and purifier is also used. Bio-NG captured during purification is
 170 combined with the produced SNG and injected into the NG grid at the same
 171 existing site used by the WAGABOX[®] unit. The project boundary is input
 172 from the electrical grid and WAGABOX[®] effluent to output to NG grid in-
 173 jection as shown in Figure 2. Normal cubic metres (Nm³) are used throughout
 174 the article to represent gas volumes in a simple, comparative fashion. The
 175 configuration as described above is known as the standard configuration in
 176 this article. Mobility options and NG grid injection capacity improvement
 177 were also investigated and will be discussed in the next subsection.

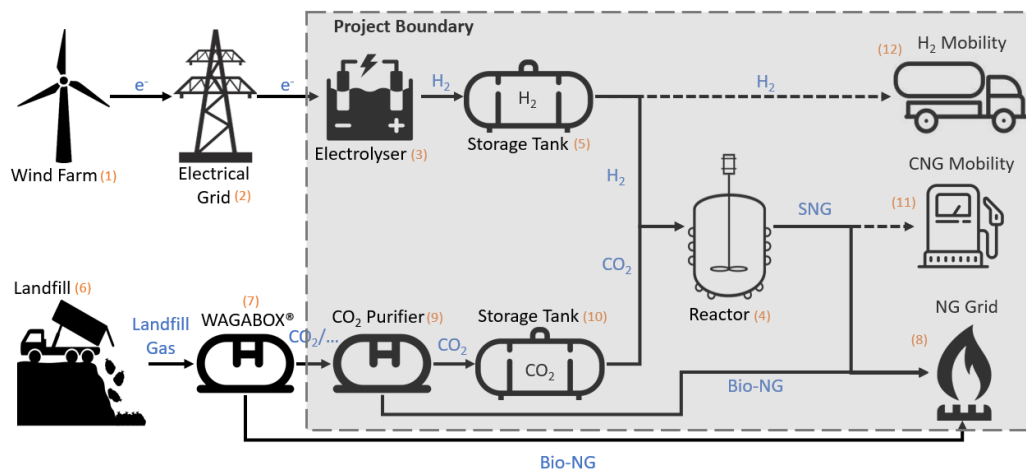


Figure 2: HYCAUNAIS project plant schematic and process flow.

178 To improve economics of the plant, participation in electricity grid ser-
 179 vices by the electrolyser is considered in all scenarios simulated, namely the

180 primary reserve or FCR. Electrolysers have been shown to be capable of
181 operating dynamically at ramping rates faster than required for FCR par-
182 ticipation [26]. FCR consumer participation is compensated according to
183 the reserve capacity in €/MW.30min in a market-based scheme, with par-
184 ticipation given in 4-hour continuous blocks. More information on ancillary
185 services are provided in [27]. Guinot et al. [28] concluded that an electrolyser
186 participating in the FCR in France was not economical with the technical and
187 economical assumptions made and current compensation values. However,
188 as stated earlier, this study will investigate the use of an innovative electrol-
189 yser stack that is capable of doubling its rated capacity for periods longer
190 than required for maximum frequency disturbance (15 minutes). This will
191 allow the operator to offer the rated capacity of the electrolyser to the FCR
192 while still operating at rated capacity, avoiding loss of hydrogen production
193 for dedicated capacity on reserve for FCR solicitation.

194 *2.2. Additional Configurations*

195 When injecting in the NG grid, knowledge of local capacity availability
196 should be known as injection may not be possible all year round. If it is not,
197 other end-use applications can be investigated to maximize the operational
198 hours of the plant. NG grid expansion, increasing the local capacity, is also a
199 possibility if the transmission systems operator (TSO) is interested in doing
200 so. One specific scenario is called a "mesh upgrade" and includes installing
201 a new pipeline between the local NG distribution grid and another grid in
202 close proximity, essentially connecting two "island" distribution grids and
203 consequently increasing both their capacities. This will be investigated as
204 a possible plant "configuration": although the equipment will be the same

205 as the standard configuration, the constraint of NG grid injection will be
206 less stringent but still applicable, allowing for more injection throughout the
207 year.

208 As seen in Figure 2, two mobility options are considered as additional
209 end-use applications: H₂ and compressed natural gas (CNG). The mobility
210 options must be designed for local transportation requirements to provide
211 realistic approximation of their demand in the model simulation. Each mo-
212 bility option will be evaluated separately as additional end-use applications
213 to the standard configuration, increasing utilization of the plant.

214 *2.3. Electricity Purchasing Contracts*

215 Two electricity purchasing contracts were investigated: long-term fixed-
216 priced contracts or short-term DA market purchasing. Long-term contracts
217 allow for operation of the plant at a specified fixed electricity price whereas
218 DA market purchasing allow plant operators to take advantage of lower
219 prices, choosing to operate when electricity prices are satisfactory as per
220 conditions set by them.

221 *2.4. Equipment Description*

222 *2.4.1. Electrolyser*

223 A 1 MW PEM electrolyser is used for the system and its modeling pa-
224 rameters are shown in Table 1. Values of parameters were either taken from
225 sources listed or the HYCAUNAS project directly. The investment cost or
226 CAPEX listed only includes the cost of the electrolyser. Balance of plant
227 (BOP) components (pumps, water purification, electronics, etc.) are in-
228 cluded as a general BOP cost to the whole plant configuration of the scenario

229 as shown in Equation 8. The electrical energy consumption of the electrol-
 230 yser is represented as a range due to its variability in its operating range.
 231 The electrolyser is assumed to be capable of responding instantaneously to
 232 changes in power consumption, so ramping is not considered. Further, as
 233 mentioned earlier, an electrolyser capable of operating up to 200% its nomi-
 234 nal capacity is considered. All values provided by the HYCAUNAIIS project
 235 and its partners are shown under Source as "project".

Table 1: PEM electrolyser model parameters.

Parameter	Unit	Value	Source
Rated power	MW _{el}	1	project
Operating pressure	bar	30	project
Electrical energy consumption	kWh/Nm ³ H ₂	4.6-5.1	[11]
Operational range	% rated power	10-200	project
Stack life	hours	60,000	[15]
Water consumption	L H ₂ O/Nm ³ H ₂	2	[29]
CAPEX	€	1,400,000	[15]
Fixed OPEX	% CAPEX/a	2	[15]
Stack replacement cost	% CAPEX	25	[15]

236 2.4.2. Methanation Reactor

237 A biological reactor capable of consuming the rated flow rate of the elec-
 238 trolyser is used – 50 Nm³/h. The model parameters used are shown in Table
 239 2. Reactor electrical consumption is due to the continuous mixing from its

240 internal propeller [30] which is assumed to be fixed when operational. Unlike
 241 electrolyzers, methanation reactors have not been shown to be capable of
 242 operating at sufficient ramping rates while still maintaining high gas quality
 243 [31]. Thus, the model considers reactor ramping when changes in gas flow
 244 rates occur. Additionally, the reactor is assumed to be fed the methanation
 245 stoichiometric ratio of $H_2/CO_2 = 4$ at all times and a fixed CO_2 conversion
 246 rate occurring inside the reactor of 98 vol% (which has been shown to be
 247 possible with transient operation [32] and applied in other studies [21]). The
 248 fixed CO_2 conversion rate and H_2/O_2 ratio is applied throughout the reactor
 249 operational range, eliminating the requirement of modelling reactor kinetics.

Table 2: Biological methanation reactor model parameters.

Parameter	Unit	Value	Source
Rated SNG capacity	Nm ³ /h	50	project
Inlet pressure	bar	16	project
Electrical energy consumption	kWh/Nm ³ SNG	1	[11]
CAPEX	€	817,500	[15]
Fixed OPEX	% CAPEX/a	5	[15]

250 2.4.3. Carbon Dioxide Purification

251 The CO_2 purification technology used is chemical scrubbing via amines
 252 due to its low pressure requirement and market availability [33]. However,
 253 it requires a heat source; it is considered to be harnessed from the reactor's
 254 exothermic heat dissipation. Model parameters used for chemical scrubbing

255 are shown in Table 3. 4% of the biogas input is bio-NG - which can be
 256 captured and mixed with the produced SNG - and 88% is CO₂. The chemical
 257 scrubbing system is sized such that it is capable of purifying the rated CO₂
 258 capacity of the reactor.

Table 3: CO₂ purification model parameters.

Parameter	Unit	Value	Source
Electrical energy consumption	kWh/Nm ³ biogas	0.15	[34]
Water consumption	L H ₂ O/Nm ³ biogas	0.032	[33]
CAPEX	€	91,200	[33]
Fixed OPEX	% CAPEX/a	3	[33]

259 2.4.4. Hydrogen Mobility

260 H₂ mobility was designed as a refilling site for tube-trailers as there is no
 261 hydrogen consumption anticipated on-site. These trailers are able to travel
 262 up to 400 km from the fill-site to refuelling stations in local regions. Some
 263 of these regions, such as Bourgogne-Franche-Comté, are planning to enlarge
 264 their fuel cell electric vehicle (FCEV) bus fleets in the coming years [35]. The
 265 distributors in these regions are assumed to be the H₂ mobility consumers.
 266 Two tube-trailers with a capacity of 400 kg each at 200 bar were used, with
 267 an assumption that at least one will be available on-site to be filled at any
 268 time. The refilling station cost was calculated using a modeled developed by
 269 [20]. H₂ mobility model parameters are shown in Table 4. The refilling site

270 was sized to be capable of receiving the rated capacity of the electrolyser.

Table 4: H₂ mobility model parameters.

Parameter	Unit	Value	Source
Tube-trailer CAPEX	€/kg	500	[20]
Tube-trailer fixed OPEX	% CAPEX/a	2	[20]
Site CAPEX	€	232,709	[20]
Site fixed OPEX	% CAPEX/a	3	[20]

271 2.4.5. Compressed Natural Gas Mobility

272 A refuelling station was assumed to be installed on-site for CNG mobility
273 which could be consumed by waste trucks used for landfill community pickup.
274 It is proposed that the fleet could be switched to operate on CNG, starting
275 with two trucks and possibly increasing in later years. However, the model
276 simulation will only assume two vehicles for the project lifespan. The trucks
277 are assumed to be filled overnight. The station is sized so that it can accept
278 the rated capacity of the reactor if NG grid injection is not possible. The
279 resulting refuelling station costs are shown in Table 5. Waste trucks are
280 not included in the cost of the station. Costs were taken from values and
281 models given in [36], which include a dispenser, time-fill post and gas dryer.
282 Compressor cost is also included in the station CAPEX.

283 2.4.6. Gas Storage

284 All tanks used in the system use the same CAPEX and OPEX param-
285 eters as listed in Table 6. The gas compressor parameters are also listed

Table 5: CNG mobility model parameters.

Parameter	Unit	Value	Source
Station CAPEX	€	232,417	[36]
Station fixed OPEX	% CAPEX/a	3	[36]

286 in this table. Intermediate H₂ storage is done at the equivalent pressure of
 287 electrolyser output, 30 bar, eliminating the need of a compressor. However,
 288 a compressor is required if H₂ mobility is considered for the tube-trailers, as
 289 described below. Intermediate CO₂ is pressurized to 16 bar to meet reactor
 290 input requirements while the CH₄ storage is at 200 bar for CNG mobility re-
 291 quirements. All tanks are assumed to have their complete capacity available
 292 for production. The electrical consumption varies greatly due to the pres-
 293 sure and gas being compressed [37]. The CAPEX of a compressor also varies
 294 greatly depending on the gas and compressor type; values for H₂ [20], CH₄
 295 [38] and CO₂ [36] were taken from their respective source. The compressor
 296 must be completely replaced at the end of their useful life, which is defined
 297 as 10 years of continuous operation [15].

298 *2.4.7. Natural Gas Grid Injection*

299 The costs associated to NG grid injection are shown in Table 7. The
 300 difference in CAPEX values is due to the increased cost for installation of
 301 the mesh pipeline to connect two distribution grids.

Table 6: Gas tank and compressor model parameters.

Parameter	Unit	Value			Source
		H ₂	CO ₂	CH ₄	
Tank capacity	Nm ³	see 3.4.4	50	600	project
Tank rated pressure	bar	30	16	200	project
Tank CAPEX	€/Nm ³	100	100	100	[15]
Tank fixed OPEX	% CAPEX/a	2	2	2	[15]
Compressor electrical consumption	kWh/kg	1.68	0.09	0.20	[37]
Compressor lifespan	hours	87,600	87,600	87,600	[15]
Compressor CAPEX	€	200,000	234,636	101,398	[20, 38, 36]
Compressor fixed OPEX	% CAPEX/a	3	3	3	[15]
Compressor replacement cost	% CAPEX	100	100	100	[15]

Table 7: NG grid injection model parameters.

Parameter	Unit	Value	Source
Grid injection CAPEX (no mesh)	€	20,500	project
Grid injection CAPEX (mesh)		252,100	project
Grid injection fixed OPEX	% CAPEX/a	8	[15]

302 2.5. Operational Scenarios

303 Eight scenarios were developed to evaluate the different plant configura-
304 tions and electricity contracts. They are listed in Table 8, with the con-
305 figuration and electricity purchasing option used marked accordingly. A

306 "standard" configuration (S1 and S5) includes SNG production for NG grid
 307 injection only. The mesh upgrade scenarios (S2 and S6) increase the NG
 308 grid capacity by installing a new pipeline to connect two "island" distribu-
 309 tion grids together whereas the mobility options (S2, S3, S6 and S7) use the
 310 standard configuration plus H₂ or CNG mobility stations. For H₂ mobility
 311 configurations, a refilling station with tube-trailers is used and consumption
 312 is only considered when SNG production is not possible. For CNG mobility
 313 configurations, a waste truck refuelling station on-site is considered which
 314 will have a continuous flow to fill the trucks daily, plus can also accept SNG
 315 production surplus when grid injection is not possible. Each configuration is
 316 tested independently to discover their individual attributes. Fixed electricity
 317 contract (S1-S4) and DA market participation (S5-S8) are also investigated
 318 for each configuration type to find what is the preferred electricity contract.

Table 8: Eight scenarios developed for project evaluation, with the type of electricity contract and configuration implemented in each scenario marked accordingly.

Scenario	Electricity Purchasing		Configurations			
	Fixed Contract	DA Market	Standard	Mesh	H ₂ Mobility	CH ₄ Mobility
S1	X		X			
S2	X			X		
S3	X				X	
S4	X					X
S5		X	X			
S6		X		X		
S7		X			X	
S8		X				X

319 Table 9 shows the equipment considered for each scenario. As can be seen
 320 and was explained earlier, all scenarios consider SNG production and NG

321 grid injection, with S2-S4 and S6-S8 also considering additional equipment
 322 to increase operational hours of the plant.

Table 9: The equipment considered for each scenarios configuration.

Equipment	S1	S2	S3	S4	S5	S6	S7	S8
Electrolyser	X	X	X	X	X	X	X	X
H ₂ tank	X	X	X	X	X	X	X	X
CO ₂ purification	X	X	X	X	X	X	X	X
CO ₂ compressor	X	X	X	X	X	X	X	X
CO ₂ tank	X	X	X	X	X	X	X	X
Reactor	X	X	X	X	X	X	X	X
Grid injection	X	X	X	X	X	X	X	X
Grid injection w/ mesh		X				X		
H ₂ compressor			X				X	
H ₂ tube-trailer			X				X	
CH ₄ compressor				X				X
CH ₄ tank				X				X
CH ₄ fuelling station				X				X

323 2.6. Analysis Metrics

324 A multi-metric analysis was done to evaluate each operational scenario.
 325 Using the analysis results, users can determine what is the preferred config-
 326 uration and electricity contract for their plant. Five metrics were analysed:
 327 levelized cost of methane (LCOM), CAPEX, minimum selling price (MSP),
 328 electrolyser OH and tank size. These metrics can be divided into economical
 329 and operational metrics, as described in the following subsections.

330 *2.6.1. Economical Metrics*

331 LCOM is a modified version of the levelized cost of energy (LCOE) which
332 calculates the production cost of each unit of energy produced in the project
333 lifespan in terms of the reference year and is a common way to compare
334 energy costs of different technologies [11]. In this case, methane is being
335 produced and the reference is the installation year (year 0). LCOM is found
336 by using Equation 1:

$$LCOM = \frac{CAPEX + C_{rep} + (OPEX + F) \cdot k_a}{Q_{SNG} \cdot k_a} \quad (1)$$

337 where: $CAPEX$ is the capital expenditure of all equipment for the simulated
338 scenario; C_{rep} represents the total levelized cost of equipment replacement
339 during the project lifespan; $OPEX$ is the operational expenditure of all
340 equipment for the simulated scenario in the first year of operation (year 1);
341 F represents the costs of plant feedstocks, namely electricity and water in
342 year 1; Q_{SNG} is the total amount of SNG production in year 1 used for
343 both CNG mobility and NG grid injection; k_a is the discount factor, used to
344 extrapolate all year 1 values over the whole project lifespan. It is calculated
345 as shown in Equation 2 below:

$$k_a = \frac{(1 + r)^n - 1}{r(1 + r)^n} \quad (2)$$

346 where r is the discount rate in % and n is the project lifespan in years. k_a is
347 used to extrapolate values from year 1 over the project lifespan, which is then
348 used in economical analysis. The values of r and n used are shown in Table
349 10. $OPEX$ can be broken down into two types of operational costs: fixed
350 ($OPEX_{fix}$) and variable ($OPEX_{var}$) and are summed as shown in Equation

351 3:

$$OPEX = \sum_{t=1}^m OPEX_{var,t} + OPEX_{fix} \quad (3)$$

352 where $OPEX_{fix}$ represents the summed fixed operational costs of all equip-
353 ment included in the simulated scenario, equal to a defined percentage of
354 the equipment CAPEX. $OPEX_{var,t}$ represents the variable cost associated
355 to operating the equipment at time step t in the set m , representing the
356 total number of time steps to simulate the calendar year. Only the reactor
357 variable costs are considered in the simulation which is associated to nutrient
358 replacement and can be found by multiplying the quantity of SNG produced
359 at time step t ($Q_{SNG,t}$) by a fixed cost of the nutrient ($c_{var,rea}$) as shown in
360 Equation 4:

$$OPEX_{var,t} = Q_{SNG,t} \cdot c_{var,rea} \quad (4)$$

361 It should be noted that variable costs associated to feedstocks are consid-
362 ered separately. Further, when considering feedstock costs F the electrical
363 consumption of electrolysis, compressors, CO₂ separation and reactor mix-
364 ing (continuously stirred tank reactor assumed to be used [30]) are included;
365 electrolysis and CO₂ separation are considered for water consumption. For
366 C_{rep} , the total number of operational hours determine when equipment must
367 be replaced, with the replacement cost equal to a determined percentage of
368 the CAPEX.

369 MSP is a metric used to include the revenue of FCR participation and
370 H₂ sold for mobility purposes as a reduction of the LCOM to determine
371 what is the minimum selling price SNG can be sold (in €/MWh) for either

372 CNG mobility or gas grid injection applications. MSP can be found by using
 373 Equation 5:

$$MSP = \frac{(OPEX + F - R_{H_2} - R_{FCR})k_a + CAPEX + C_{rep}}{Q_{SNG} \cdot k_a} \quad (5)$$

374 where R_{H_2} and R_{FCR} are the revenue from H_2 mobility and FCR, respectively,
 375 in year 1. It can be seen that besides the inclusion of these revenues the rest
 376 of the equation is identical to the LCOM equation. R_{H_2} is found by Equation
 377 6:

$$R_{H_2} = \sum_{t=1}^m Q_{H_2, mob, t} \cdot v_{H_2} \quad (6)$$

378 where $Q_{H_2, mob, t}$ is the quantity of H_2 used for mobility at time step t and
 379 v_{H_2} is the price value of hydrogen for mobility in €/kg. $R_{FCR, t}$ is generated
 380 only if the electrolyser is participating in the FCR during the time step t as
 381 shown in Equation 7:

$$R_{FCR} = \sum_{t=1}^m sig_{FCR, t} \cdot v_{FCR} \cdot P_{r, elect} \quad (7)$$

382 where $sig_{FCR, t}$ is a signal indicating if the electrolyser is active in the FCR
 383 at time step t ($sig_{FCR, t} = 1$ if participating and $sig_{FCR, t} = 0$ is not partici-
 384 pating), v_{FCR} is the price value of participating in the FCR in €/MW/h and
 385 $P_{r, elect}$ is the rated power of the electrolyser in MW.

386 $CAPEX$ is the total capital costs of all equipment in the simulated sce-
 387 nario multiplied by an additional balance of plant (BOP) cost - design, en-
 388 gineering, and other additional costs - as shown Equation 8:

$$CAPEX = CAPEX_{equip} \cdot (1 + c_{BOP}) \quad (8)$$

389 where $CAPEX_{equip}$ is the total CAPEX of all equipment included in the
 390 simulated scenario and c_{BOP} is the BOP cost. Although CAPEX is included
 391 in the calculation of the other economical metrics, it is valuable to evaluate
 392 independently to appreciate the initial cost required for plant construction.

393 2.6.2. Operational Metrics

394 OH of the electrolyser or OH_{elect} is the total of partial, rated and overload
 395 operational hours of the electrolyser in the year. It is use as a metric gives
 396 insight into the effect OH has on the levelized cost and how much operation
 397 is required to obtain those costs.

398 Intermediate hydrogen tank size is determined independently from the
 399 main model for each scenario to give the lowest MSP. This will ensure that
 400 the tank is not oversized and increase the investment cost without any eco-
 401 nomical benefit. The resulting capacity will determine the duration of storage
 402 capable for the configuration: larger tanks can prolong production in times
 403 of unfavorable hydrogen production and allow continuous reactor operation;
 404 smaller tanks will require indeterminacy in reactor operation, more closely
 405 following electrolyser operation.

406 A scaled comparison of the key metrics in each scenario is helpful for
 407 analysis. Once scaled in a defined range $[a, b]$, the ranking of each scenario's
 408 metric value can be compared. This can be done by normalizing each scenario
 409 metric using Equation 9:

$$x_{i,n} = (b - a) \frac{x_i - \min(x_i)}{\max(x_i) - \min(x_i)} + a \quad (9)$$

410 where: x_i is equal to metric i 's value of each scenario; $x_{i,n}$ is the normalized
 411 value of metric i in each scenario and $\min(x_i)$ and $\max(x_i)$ are the minimum
 412 and maximum scenario value of metric i . This equation will rank values
 413 such that the highest value in each metric receives the highest rank. If the
 414 lowest value of the metric should be ranked the highest, the equation must
 415 be slightly modified as in Equation 10:

$$x_{i,n} = (b - a) \left(1 - \frac{x_i - \min(x_i)}{\max(x_i) - \min(x_i)} \right) + a \quad (10)$$

416 2.7. Model Constraints

417 Constraints of model variables must be defined for model operation.
 418 $Q_{SNG,t}$ should not be higher than the current local NG grid consumption
 419 ($cons_{grid,t}$) for every iteration t in the simulation. If it is, there is no capacity
 420 available for grid injection. This is shown in Equation 11:

$$Q_{SNG,t} \leq cons_{grid,t} \quad (11)$$

421 A maximum yearly operational hours must be defined for the electrolyser
 422 ($OH_{max,elect}$) and reactor ($OH_{max,rea}$) in the simulation to allow for mainte-
 423 nance. These constraints are shown in Equations 12 and 13:

$$OH_{elect} \leq OH_{max,elect} \quad (12)$$

$$OH_{rea} \leq OH_{max,rea} \quad (13)$$

424 where OH_{elect} and OH_{rea} are the total yearly operational hours of the elec-
 425 trolyser and reactor, respectively. The electrolyser and reactor must also
 426 operate within their allowable production limits. For the electrolyser this is
 427 defined by its electrical power consumption while the reactor is defined by
 428 its hydrogen consumption. This is shown in Equations 14 and 15:

$$P_{elect,min} \leq P_{elect,t} \leq P_{elect,max} \quad (14)$$

$$Q_{H_2,rea,min} \leq Q_{H_2,rea,t} \leq Q_{H_2,rea,max} \quad (15)$$

429 where $P_{elect,min}$ and $P_{elect,max}$ are the minimum and maximum operational
 430 power consumption of the electrolyser, respectively, and $P_{elect,t}$ is the opera-
 431 tional power consumption at time step t . $Q_{H_2,rea,min}$ and $Q_{H_2,rea,max}$ are the
 432 minimum and maximum hydrogen consumption of the reactor, respectively,
 433 and $Q_{H_2,rea,t}$ is the hydrogen consumption of the reactor at time step t . The
 434 hydrogen tank pressure must be within its minimum and rated pressure, as
 435 shown in Equation 16:

$$p_{min,tank} \leq p_{tank,t} \leq p_{r,tank} \quad (16)$$

436 where: $p_{tank,t}$ is the hydrogen pressure in the tank at time step t ; $p_{r,tank}$
 437 is the rated pressure capacity and $p_{min,tank}$ is the minimum tank pressure.
 438 Ramping for the electrolyser was assumed to be instantaneous as explained
 439 in 2.1; the reactor could not be assumed to do so. Two different ramping
 440 rates were used for the reactor depending upon the hydrogen flow rate to the
 441 reactor: above or below rated capacity. This is expressed in the conditional
 442 Equation 17:

$$rr_{rea} = \begin{cases} rr_{rea,below}, & \text{if } Q_{H_2,rea,t} \leq Q_{r,H_2,rea} \\ rr_{rea,above}, & \text{if } Q_{H_2,rea,t} \geq Q_{r,H_2,rea} \end{cases} \quad (17)$$

443 where $rr_{rea,below}$ and rr_{above} is the ramping rate below and above reactor rated
444 capacity, respectively. The ramping rate values are sensitive to the project
445 partner and thus cannot be listed. The electrolyser will ideally operate at
446 rated power continuously for maximum production and reduced wear on the
447 equipment. Further, as the profitability of the plant is the primary objective,
448 participating in the FCR should be maximized. To be able to participate at
449 100% rated capacity, the electrolyser must be operating at rated capacity to
450 offer a symmetrical reserve. Therefore, continuous operation of the electrol-
451 yser at rated capacity is desired, as long as other system limitations allow it.
452 To keep the carbon intensity of the plant minimized, the plant is said to be
453 following the wind profile whenever total power output from the wind farms
454 is above rated capacity of the electrolyser; if not, it will purchase from other
455 sources on the grid. As France's power generation is over 87% low-carbon
456 and 22% renewable [39] as of 2019, the gases could still be considered "green"
457 depending on the definition, but is certainly low-carbon. This consideration
458 for power source is shown in Equation 18:

$$P_{elect,t} = \begin{cases} P_{wind,t}, & \text{if } P_{wind,t} \geq P_{r,elect} \\ P_{grid,t}, & \text{else} \end{cases} \quad (18)$$

459 where $P_{wind,t}$ is the the electrical power of the wind farm at time step t and
460 $P_{grid,t}$ is electrical power sourced from other grid sources. When considering
461 DA market electricity prices (S5-S8), it is beneficial to operate only when
462 electricity prices favor production. This can be defined as the willingness to

463 pay (WTP) for electricity: if the electricity price is above a certain value,
 464 the operator of the plant will choose not to run production; if the price is
 465 below that value the plant will operate. In the short-term, this value would
 466 be determined by the marginal profit of the plant at each hour whereas in
 467 the long-term, total costs and revenues must also be considered [40]. For the
 468 purposes of the model, a range of electricity prices will be used to find the
 469 optimal WTP for plant operation in each scenario: if the variable cost of
 470 electricity at time step t ($c_{el,t}$) is lower than or equal to the pre-determined
 471 WTP (WTP_{det}), the electrolyser will operate at the determined power level;
 472 if WTP_{det} is larger than $c_{el,t}$, the electrolyser will sit idle. This is expressed
 473 in Equation 19:

$$P_{elect,t} = \begin{cases} P_{elect,t}, & \text{if } c_{el,t} \leq WTP_{det} \\ 0, & \text{else} \end{cases} \quad (19)$$

474 As electrolyser and reactor operation are decoupled due to intermediate hy-
 475 drogen storage, the reactor may still be producing if the electrolyser is sitting
 476 idle: reactor operation depends on hydrogen availability in the storage tank
 477 and not hydrogen production. When participating in the FCR, the electrol-
 478 yser power has a further constraint such that it must follow the frequency of
 479 the grid: when the frequency is below 50 Hz, less power must be consumed
 480 to bring it back to balance; when the frequency is above 50 Hz, more power
 481 must be consumed. This relationship can be expressed in Equations 20 and
 482 21:

$$P_{FCR,t} = sig_{FCR,t} \cdot K(f_t - f_n) \quad (20)$$

$$P_{elect,tot,t} = P_{elect,t} + P_{FCR,t} \quad (21)$$

483 where $P_{FCR,t}$ power adjustment of the electrolyser at time step t in MW; K
 484 is the FCR gain as defined by the TSO (RTE) for the consumption site in
 485 MW/Hz [41]; f_t is the measured grid frequency at time step t in Hz; f_n is
 486 the nominal grid frequency in Hz and $P_{elect,tot,t}$ is the total electrolyser power
 487 consumption at time step t . Note that $P_{FCR,t}$ can be negative or positive,
 488 depending on the grid frequency measured at that time step.

489 *2.8. Operational Strategy*

490 Operational strategies when mobility is included as an extra end-use ap-
 491 plication is required. For H₂ mobility configurations, a refilling station with
 492 tube-trailers is used and consumption is only considered when SNG pro-
 493 duction is not possible. For CNG mobility configurations, a waste truck
 494 refuelling station on-site is considered which will have a continuous flow to
 495 fill the trucks daily, plus can also accept SNG production surplus when grid
 496 injection is not possible.

497 A continuous flow rate from the reactor to the refuelling station is as-
 498 sumed that is equal to the estimated yearly mileage and fuel efficiency of a
 499 CNG waste truck as proposed by [42] and shown in Equation 22:

$$Q_{CNG,r} = \frac{n_{trucks}(35Nm^3/100km)(20,000km/year)}{8760h} \quad (22)$$

500 where $Q_{CNG,r}$ is the hourly SNG production to the refuelling station and
 501 n_{trucks} is the number of CNG waste trucks.

502 The constraints and assumptions presented above provide the framework
 503 for operation simulation. The model begins operation with variable input

504 data and defined parameters, performing a loop of one year in defined time
505 steps. Logic controllers determine the flow of model execution at each iter-
506 ation, inputting the required data to modules representing the plant equip-
507 ment. These equipment modules compute their production costs and resul-
508 tant gas flow rates, inputting them into the next controller or to the final
509 module for economical analysis.

510 The time step used for modeling is 10-minutes to equal the resolution
511 of data given for the wind farm power profile for an entire year, equaling
512 52,560 time steps performed by the simulation. Further, a maximum oper-
513 ational time of 95% of the year was chosen for the electrolyser and reactor
514 ($OH_{max,elect} = OH_{max,rea} = 8322$), allowing some hours during the year for
515 operational maintenance.

516 *2.9. Economical Parameters*

517 The economical parameters used for modeling are shown in Table 10. It
518 was assumed that a fixed electricity contract of 65 €/MWh could be attained
519 for the duration of the project. A local fixed water price is used for the
520 model [43]. Enumeration for electrolysers in the FCR is based upon the DA
521 market reserve price, with payment given to each MW for the bid duration.
522 Historical data is provided by [44], given in €/MW/30min. Between 2016-
523 2019, hourly prices have fluctuated between 4-20 €/MW/h, with the average
524 in 2019 being 9 €/MW/h. The price of H₂ sold to distributors (refuelling
525 stations) is taken from [20]. A discount rate of 7% and project lifespan of 20
526 years are used.

Table 10: Economical model parameters.

Parameter	Unit	Value	Source
Fixed electricity price	€/MWh	65	project
Water cost	€/m ³	1.60	[43]
BOP (c_{BOP})	% CAPEX	40	[15]
FCR participation price	€/MW/h	9	[44]
H ₂ selling price (distributor)	€/kg	7	[20]
Discount rate (r)	%	7	project
Project lifespan (n)	years	20	project

527 *2.10. Sensitivity Analysis*

528 A sensitivity analysis is performed to visualize the influence of various
 529 input values. The values chosen to be investigated are: electricity price, gas
 530 grid availability, electrolyser efficiency and electrolyser and reactor CAPEX.
 531 The sensitivity analysis is chosen to be done on the most favourable scenarios
 532 as chosen during the analysis of the key metrics.

533 **3. Results and Discussion**

534 An analysis of model inputs is done first to understand what limitations
 535 and opportunities they provide. This includes: electricity price, local gas
 536 consumption and wind power. The key parameters results for each scenario
 537 in 2017 and 2018 will then be analysed, determining the advantages and
 538 disadvantages of the configurations and where improvements are needed to
 539 give more favorable results.

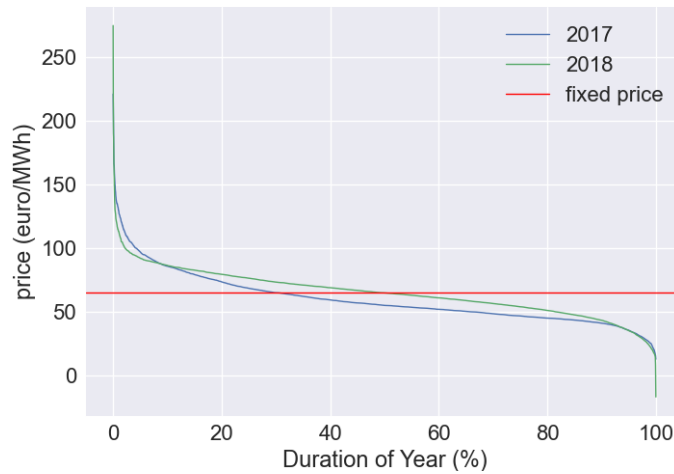
540 *3.1. Electricity Price Analysis*

541 As electricity is the most costly part of power-to-gas operation, an anal-
542 ysis of DA market SPOT electricity prices over the year can give important
543 operational insights. Figure 3a shows the average daily price variance over
544 2017 and 2018. A price duration curve - a curve showing the distribution of
545 electricity prices by its frequency in the year - for 2017 and 2018 are shown
546 in Figure 3b and include the taxes, fees, levies and wholesale price. The
547 fixed price used is also represented as a horizontal line for reference. We can
548 see the the average price of 2018 is roughly equal to the fixed price (64.8
549 €/MWh) while 2017 is lower at 59.57 €/MWh, suggesting lower operational
550 costs are possible in the DA market but this can vary by year.

551 To determine how the variability of price will effect operational costs, 6
552 WTP_{det} values were tested: 55, 65, 75, 85, 95 and 105 €/MWh. Based upon
553 these "cut-off" prices, the maximum amount of possible operational hours
554 for the year (shown as the duration of the year) and the average electricity
555 price for those available hours can be found. They are shown in Table 11.
556 It can be seen that at 55-65 €/MWh, the duration of the year possible for
557 operation varies greatly by year, but then converge at around 85 €/MWh.
558 This suggests great variability by year in operation (27-71%) if lower WTP_{det}
559 values are used, greatly influencing the production costs of the plant. Further,
560 it can be seen that the average price is never higher than the fixed price
561 used, meaning lower overall electricity prices when participating in the DA
562 market. To determine the ideal WTP_{det} , the scenarios were simulated with
563 each WTP_{det} value to see their respective LCOM. The result for S5 in 2017
564 is shown in Figure 4 as well as the relationship to OH. As can be seen,



(a) Average DA market SPOT price over the year.



(b) SPOT price duration curve.

Figure 3: DA market SPOT price for 2017 and 2018 represented by its yearly distribution and duration of the year; the fixed price is also shown for reference.

565 the WTP_{det} is very influential on operational costs at lower values, but has
 566 little impact past 85 €/MWh. All scenarios in both years have the same
 567 relationship as described above for S5. Therefore, a WTP_{det} of 95 €/MWh
 568 was used for all DA electricity price scenarios (S5-S8) to minimize production

569 costs and allow for the possibility of maximum yearly operational time (95%)
 570 during the simulation.

Table 11: The duration of year and average electricity price for each WTP_{det} .

WTP_{det} (€/MWh)	2017		2018	
	Duration of year (%)	Avg price (€/MWh)	Duration of year (%)	Avg price (€/MWh)
55	50.64	45.37	27.58	43.67
65	70.61	49.39	51.54	51.4
75	81.47	52.06	73.40	56.86
85	89.55	54.56	88.88	60.87
95	94.60	56.42	96.46	63.01
105	96.94	57.47	98.50	63.84

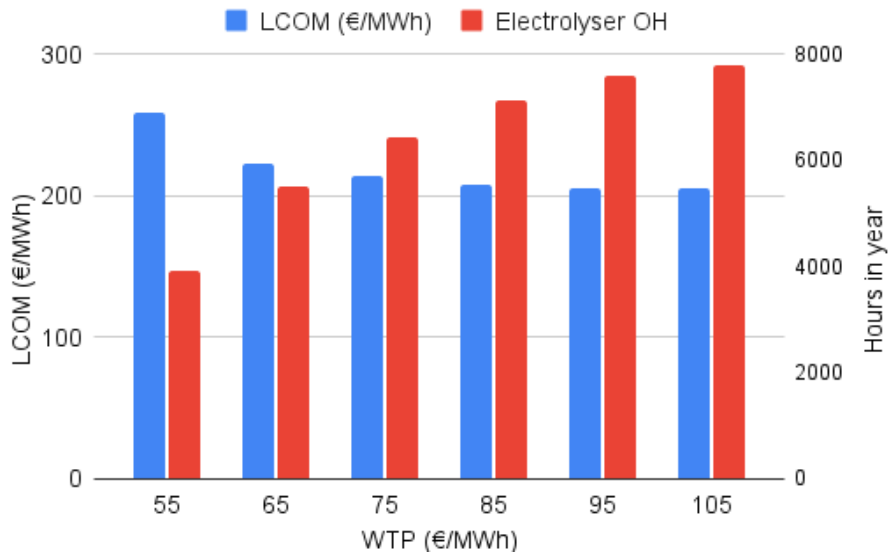


Figure 4: WTP_{det} versus LCOM and electrolyser OH for S5 in 2017.

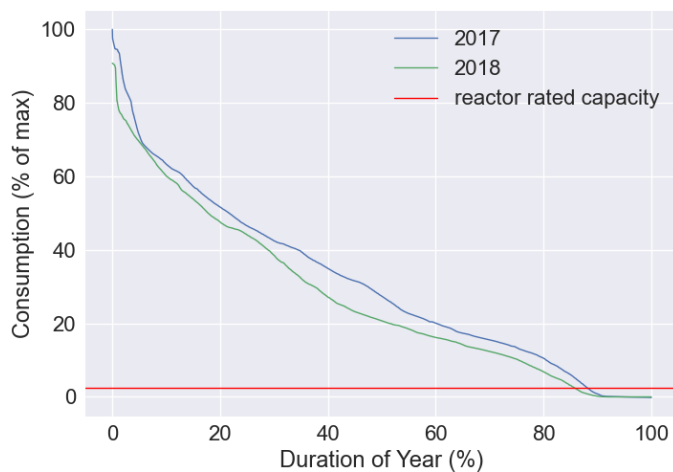
571 3.2. Gas Consumption Analysis

572 A study performed by the grid operator for the project revealed that
 573 SNG production could not be injected into the local grid year-round: at

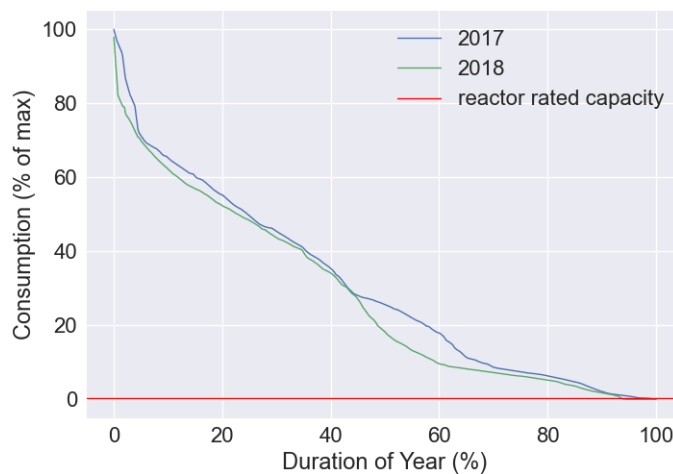
574 certain times of the year, namely summer months, there was not enough
575 (close to zero) NG consumption to allow for grid capacity to be available for
576 SNG injection. Local NG distribution network consumption determines the
577 availability of gas grid capacity for SNG injection: as long as consumption
578 is greater than SNG production, injection can take place. If not, the SNG
579 must be used elsewhere, stored or not produced at all. This condition is
580 very site-specific as consumption depends on many factors, such as: number
581 of consumers, types of consumers, capacity of network, etc. If the duration
582 curves are plotted for each year with and without the mesh and compared to
583 the reactor rated capacity, as shown normalized in Figure 5, the amount of
584 time in the year injection can take place is clearly seen: 86-88% without mesh
585 and 94-98% with mesh. When a mesh upgrade is not installed, there will be
586 many hours throughout the year where injection cannot take place, mainly in
587 the summer months. This suggests additional end-use applications could be
588 favorable to increase plant utilization, as long as their costs outweigh their
589 benefits. It would be difficult to apply the same logic when the mesh upgrade
590 is installed as there are very little hours in the year, if any, left to justify the
591 additional investment.

592 *3.3. Wind Power Analysis*

593 The wind farm power profiles are to be followed virtually by the elec-
594 trolyser, via a connection to the grid. Data for two wind farms for a total
595 capacity of 24 MW was provided by a project partner. The maximum amount
596 of wind power utilization is desired to produce green hydrogen. Analysing
597 the wind power profiles produced from the two wind farms in each year will
598 give insights into how much of H₂ production can be produced from virtually



(a) Without mesh upgrade.



(b) With mesh upgrade.

Figure 5: Local NG network consumption normalized duration curve for 2017 and 2018 with and without the mesh upgrade; reactor rated capacity is also shown as a constant production.

599 following the wind power profile over the year, determining the "greenness"
 600 of the gas. Figure 6a shows the normalized average daily total wind power
 601 for 2017 and 2018. The high variability of wind power can easily be seen.

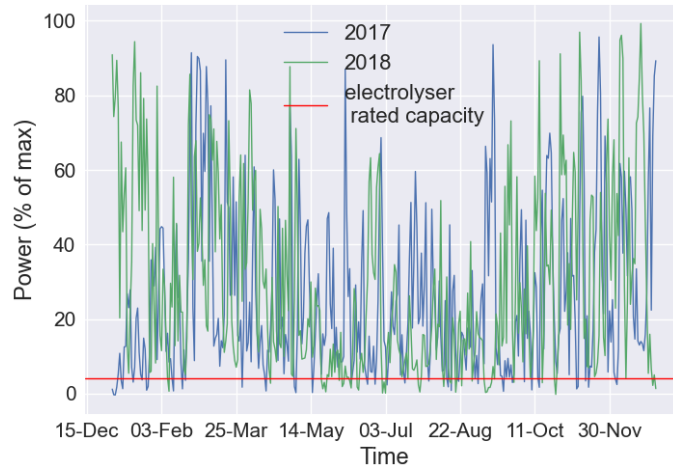
602 with lower production in the warmer months. Fortunately, the total rated
603 capacity of the wind farms is significantly higher than the electrolyser rated
604 capacity, allowing for majority of gas production to be done with renew-
605 able electricity. Indeed, the wind power exceeds electrolyser rated capacity
606 for roughly 75% of the year in 2017 and 2018 as can be seen in normalized
607 Figure 6b.

608 3.4. Results of Key Metrics

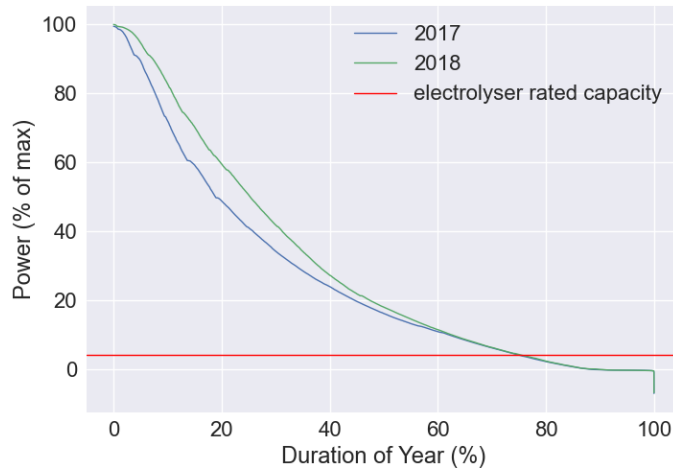
609 The key metric results are shown in Table 12 for each scenario in 2017
610 and 2018. Each metric will be discussed independently in the following sub-
611 sections.

Table 12: Key metric results for each scenario by year. The minimum values for LCOM, MSP and CAPEX are highlighted green and maximum highlighted red, as a lower value is desired. The maximum values in OH_{elect} and tank size are highlighted green and minimum highlighted red, as a higher value is desired.

Scenario	LCOM (€/MWh)	MSP (€/MWh)	OH_{elect} (hours)	H_2 Tank Size (Nm ³)	CAPEX (€)
2017					
S1	213.19	183.24	8,031	215	3,411,242
S2	218.07	188.28	8,322	130	3,723,582
S3	262.25	204.73	8,322	50	4,553,934
S4	216.67	186.91	8,322	50	3,721,956
S5	205.60	175.79	7,587	325	3,426,642
S6	204.38	174.60	8,264	175	3,729,882
S7	247.15	189.47	8,275	120	4,563,734
S8	202.67	172.91	8,287	120	3,731,756
2018					
S1	213.33	183.36	8,035	215	3,411,242
S2	218.95	189.06	8,322	130	3,723,582
S3	268.16	204.62	8,322	50	4,553,934
S4	216.62	186.88	8,322	50	3,721,956
S5	213.24	183.35	7,767	325	3,426,642
S6	218.79	188.97	8,052	175	3,729,882
S7	264.87	201.31	8,322	120	4,563,734
S8	214.27	184.48	8,303	120	3,731,756



(a) Average daily total wind power over the year.



(b) Wind power duration curve.

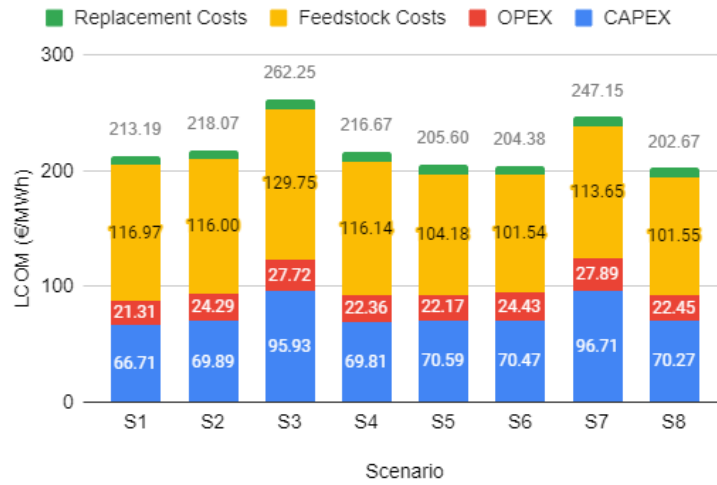
Figure 6: Total wind power for 2017 and 2018 normalized and represented by its yearly distribution and duration of the year; electrolyser rated capacity is also shown as a constant production.

612 *3.4.1. Levelized Cost of Methane*

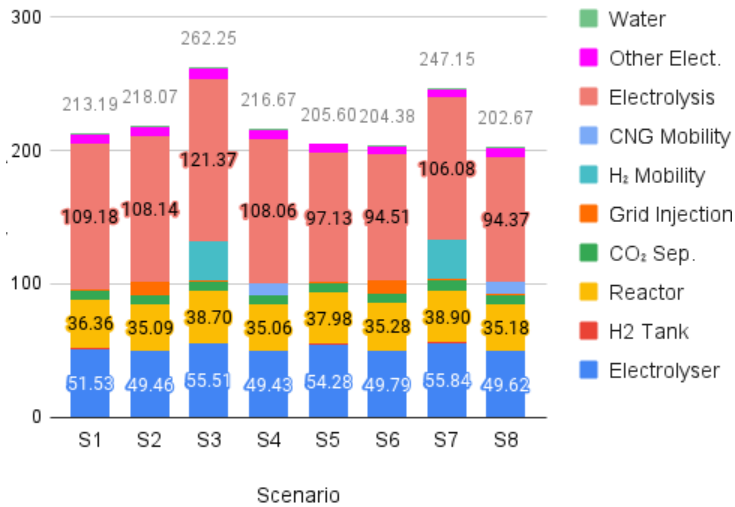
613 The LCOM for fixed electricity price scenarios (S1-S4) for 2017 and 2018
 614 are very similar, while DA pricing scenarios (S5-S8) can vary significantly by

615 year, with S7 having the largest difference at 17 €/MWh. This relationship
616 between the years is attributed to the difference in DA electricity prices,
617 showing its impact on production costs. Figure 7 shows a breakdown of the
618 LCOM by cost type and also by equipment or electricity type, with the top
619 three contributors in each breakdown value shown. Fuel costs includes water
620 and electricity as CO₂ is free in the project. As the water cost is almost
621 negligible, fuel costs essentially represents the cost of electricity, which is
622 46-55% of the LCOM, depending on the scenario. Electricity cost is less
623 in S5-S8, which is due to the lower average electricity price as described in
624 section 3.1. The reason for such a high cost proportion for electricity is water
625 electrolysis to produce H₂, which accounts for 43-51% of LCOM, depending
626 on the scenario. The next highest costs by equipment are the electrolyser
627 and reactor, respectively, due to their high CAPEX.

628 The lowest LCOM is CNG mobility with NG injection (S8) in 2017 and
629 only NG injection (S5) in 2018, with both scenarios' LCOM similar in both
630 years. This result suggests a tradeoff between these configurations: if more
631 operational hours of the plant are desired and the additional upfront costs of
632 CNG mobility can be attained, it is an attractive option. However, S6 also
633 has a low LCOM in both years, suggesting the mesh upgrade investment can
634 payoff. This may be preferred as increased gas grid injection has a lower
635 risk in terms of offloading product gas as grid injection is guaranteed to be
636 available – as long as local consumption allows it, which is almost always
637 the case with the mesh upgrade – whereas gas sold for CNG mobility is
638 dependent upon immediate local needs for transportation. Further, it can
639 be seen that LCOM of S1 is comparatively low in 2018 to almost all the DA



(a) LCOM grouped by cost type.



(b) LCOM grouped by equipment or electricity type.

Figure 7: Stacked column charts of the LCOM for each scenario in 2017 grouped by cost type and equipment or electricity type.

640 price scenarios (S5, S6 and S8). This is caused by two factors: the higher
 641 average electricity price and gas grid availability for the year.

642 The highest LCOM is always when H₂ mobility is considered (S3 and S7).

643 This is due to its very high capital costs, namely the refilling site and tube-
644 trailers. However, this can be slightly misleading as the LCOM is considering
645 the levelized costs per unit energy of methane, which would be produced less
646 in this configuration as the H₂ is used for mobility instead (when producing
647 SNG is not possible). The revenue gained from H₂ mobility also needs to be
648 considered to see if the additional investment is justified.

649 *3.4.2. Minimum Selling Price*

650 As shown in Equation 5, MSP subtracts H₂ mobility and FCR partic-
651 ipation revenue from LCOM, providing the minimum price produced SNG
652 would need to be sold at to break-even on the project. As seen in Table 12,
653 the most favorable scenarios from LCOM analysis are also the same for MSP.
654 It is interesting to investigate the influence the additional revenue streams
655 have on reducing the MSP of SNG which is done by first taking the dif-
656 ference between LCOM and MSP and computing each revenues' portion of
657 this LCOM reduction. This difference is shown graphically in Figure 8 with
658 each revenue type highlighted. As one can see, the reduction in LCOM by
659 FCR revenue is roughly the same for every scenario and year (29.73-34.20
660 €/MWh); this is due to electrolyser operational hours of the plant being very
661 similar in every scenario (discussed later in section 3.4.3). As the electrolyser
662 is participating in the FCR whenever it is operational, revenue is directly cor-
663 related to electrolyser OH (see Equation 7). When H₂ mobility is considered,
664 the reduction in LCOM is almost doubled (up to 63.56 €/MWh), which only
665 consumes about 11% of yearly H₂ production. This highlights the premium
666 paid for H₂ in mobility applications and its reason for being the main applica-
667 tion of renewable H₂ production. However, the MSP in H₂ mobility scenarios

668 (S3 and S7) are still higher than all other scenarios despite this doubling in
 669 LCOM reduction. This can be attributed to the high CAPEX associated to
 670 H₂ mobility (discussed in section 3.4.5).

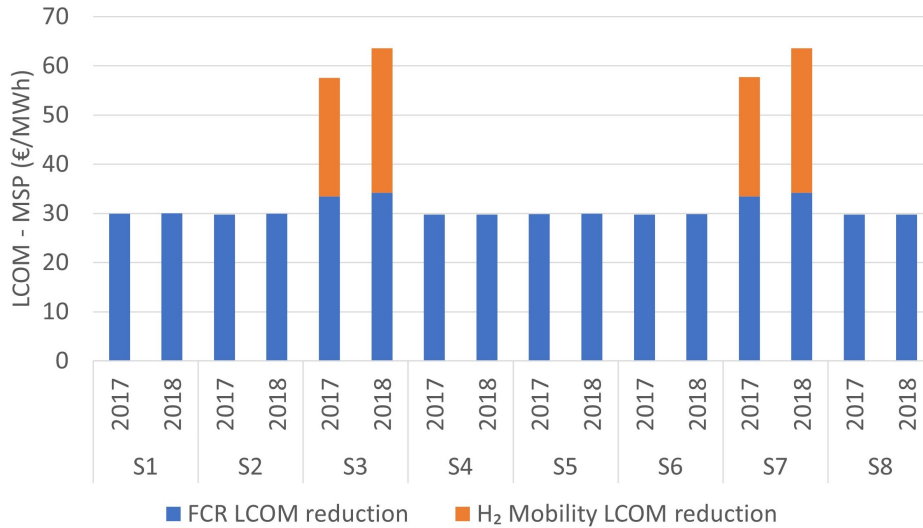


Figure 8: Difference between LCOM and MSP broken down by revenue type for each scenario and year.

671 Selling prices of 172.91-204.73 €/MWh for produced SNG are high when
 672 compared to the wholesale price of NG on the spot market at around 20
 673 €/MWh [45]. Bio-NG is currently sold and injected into the French NG grid
 674 via fixed tariffs between the producer and gas supplier for a fixed term at a
 675 price between 45-139 €/MWh depending upon the biogas source and pro-
 676 duction capacity [24]. However, as per the multiannual energy programming
 677 (PPE), these tariffs are to be reduced to a target price of 75 €/MWh by 2023
 678 and 60 €/MWh by 2028 [46]. SNG is currently not given any government
 679 support as it is a relatively new product which has been implemented in only
 680 3 projects in France at the time of writing with power ratings no greater than

681 1 MW [3]. The results presented clearly show a necessity for SNG to receive
682 a similar tariff scheme as bio-NG, with arguably higher rates. Depending
683 on plant configuration, Bio-NG production may only require biogas upgrad-
684 ing equipment while SNG production requires costly H₂ and CH₄ conversion
685 equipment, numerous gas storage mediums and CO₂ capture and possibly
686 purification technology.

687 FCR participation as a secondary revenue stream is very attractive, espe-
688 cially when using the innovative electrolyser technology allowing 200% rated
689 capacity operation for short durations, allowing no sacrifice on rated capac-
690 ity to normal operation. It provided a 29.73-34.20 €/MWh or 13.6-24%
691 reduction in LCOM, significantly impacting the MSP of SNG.

692 3.4.3. Yearly Operational Hours

693 Electrolyser OH (OH_{elect}) is high for all scenarios, between 7,587 and
694 8,322 as shown in Table 12. A fixed electricity price (S1-S4) allows electrol-
695 yser production to only be limited by tank capacity while the high WTP_{det}
696 of 95 €/MWh used in DA price scenarios (S5-S8) hardly limits production.
697 This can be seen especially if looking at the scenarios with the lowest OH:
698 NG injection only (S1 and S5). OH_{elect} and OH_{rea} are shown in Table 13 and
699 a count of the hours maximum tank capacity (tank_{cap}) stopped electrolyser
700 production and grid injection capacity (grid_{cap}) prohibited reactor operation.
701 As hydrogen storage is considered in the plant, operation of the electrolyser
702 and reactor are decoupled and thus these restrictions only limit the directly
703 affected component. As electricity price is not a constraint in S1, the sum-
704 mation of OH_{elect} and tank_{cap} equals the total hours in a year (8760) as does
705 OH_{rea} and grid_{cap}. However, in S5, the additional constraint of WTP_{det} =

706 95 €/MWh reduces OH_{elect} by about 300-500 hours per year. This reduction
 707 has a ripple effect on reactor operation due to the small tank sizes.

Table 13: Operational hours of electrolyser and reactor for the NG injection scenarios (S1 and S5) in each year, showing their limitations and portion of wind power.

Scenario	Year	OH_{elect}	Tank_{cap}	OH_{rea}	Grid_{cap}	$\text{OH}_{\text{elect,wind}}$
S1	2017	8,031	728	7,831	929	6065
	2018	8,035	725	7,655	1,105	6,110
S5	2017	7,587	699	7,384	929	5,790
	2018	7,767	683	7,425	1,105	6,267

708 A general trend of lower OH can be seen in scenarios using the DA market
 709 prices, attributed to the more flexible operation to take advantage of lower
 710 electricity prices. One final point is the amount of OH_{elect} which virtually fol-
 711 lowed the wind power profile, as shown in Table 13: 75-81% of the presented
 712 scenarios electrolyser consumed power. The other scenarios fall in this same
 713 range, showing a high majority of renewable power used for H_2 production.

714 3.4.4. Tank Size

715 Tank sizes were optimized for each scenario in terms of minimizing LCOM
 716 and are shown in Table 12. The same sizes were used in both years to compare
 717 its effect in each year and simplify modeling. The largest size is found in S5
 718 (NG injection only) which is equal about 1.5 hours of electrolyser operation,
 719 meaning longer storage of days or seasonally is not economically attractive
 720 for this project. This is largely based upon the high grid injection availability
 721 year-round. Further, the mobility scenarios have minimal storage due to their

722 independent higher pressure storage on-site of their respective stations.

723 *3.4.5. CAPEX*

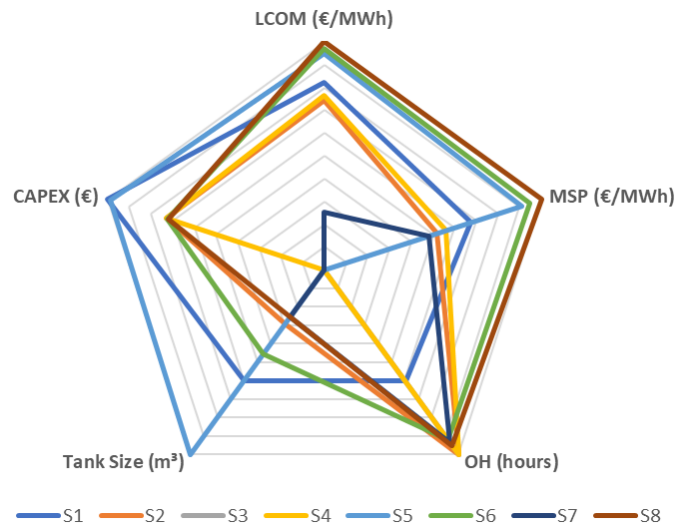
724 The CAPEX of all scenarios for both years are the same as the equip-
725 ment does not change. As stated previously, S2-S4 and S6-S8 have equipment
726 which is added to S1 and S5, respectively, to increase SNG production, mean-
727 ing a higher CAPEX. As would be expected, the standard configuration (S1)
728 has the lowest CAPEX due to its limited amount of equipment compared
729 to other scenarios. The H₂ mobility scenarios (S3 and S7) have the highest
730 CAPEX due to the current high capital cost of equipment required, namely
731 the tube-trailers, refilling site and compressor.

732 *3.4.6. Key Metric Spider Chart Comparison*

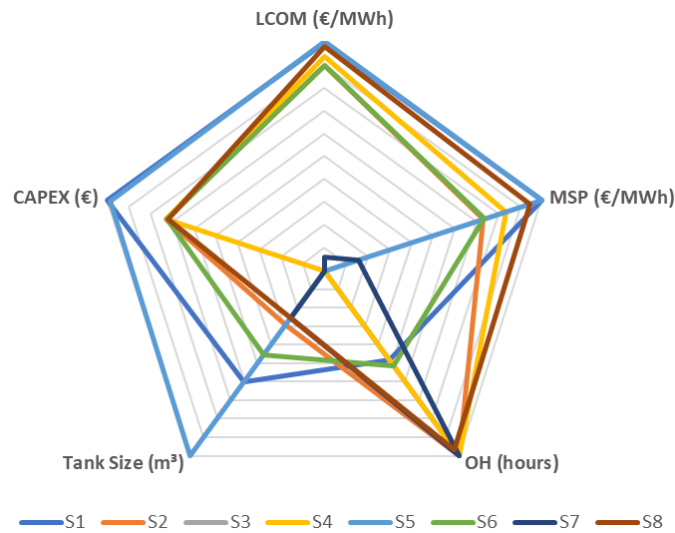
733 A scaled visual comparison of the key metrics can be done using Equations
734 9 and 10. For the operational metrics – OH_{elect} and H₂ tank size – the largest
735 value was ranked the highest whereas the economical metrics – LCOM, MSP
736 and CAPEX – the lowest value was ranked the highest. Using a range =
737 [0, 5], the spider charts shown in Figure 9 were generated showing the scaled
738 values of the metrics for each scenario and year.

739 Using this figure and the previous sections, the most interesting scenarios
740 for this project are S5 and S8 – using variable DA market electricity prices
741 with either the standard configuration or including a CNG mobility station
742 on-site. It should be noted that the difference in input data for each year
743 caused considerable changes in each scenario’s LCOM and MSP - the most
744 important metrics to consider for project feasibility studies.

745 It should be noted that CNG mobility being one of the best configura-



(a) 2017



(b) 2018

Figure 9: Spider charts of the key metrics for each year.

746 tions should be taken with caution. For modeling purposes, a continuous
 747 flow rate of SNG is sent to the station equal to two waste trucks' yearly
 748 consumption. Further, extra SNG production not accepted by the grid is

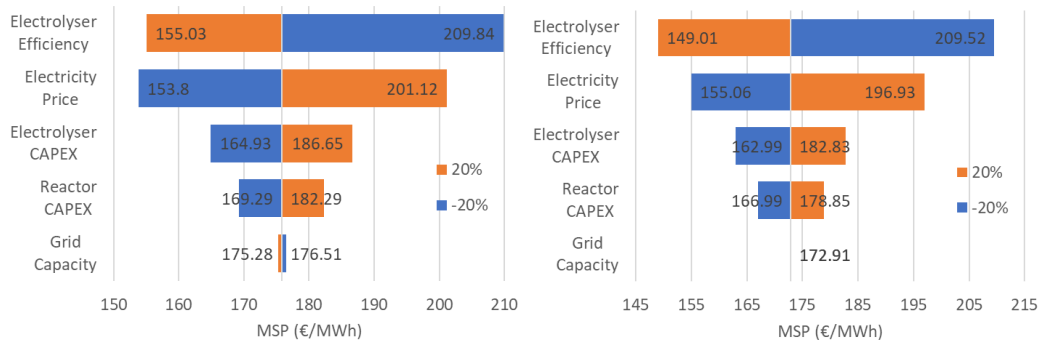
749 sent to the station, which is assumed to be consumed in some fashion by
750 increased truck consumption. This volatility in consumption, portrayed very
751 favorably in modeling, does not provide guaranteed revenue like grid injection
752 would in real-world applications. In addition, CNG mobility stations
753 are normally connected to the gas grid instead of directly to production sites
754 as modeled here; this presents uncertainty in tariffs being applied to SNG
755 sold for mobility in this configuration.

756 The attractiveness of hydrogen mobility could be seen in the results presented,
757 as other sources have also confirmed as currently the best market for power-to-gas
758 [20, 17, 19]. However, the plant studied used mobility as a secondary application
759 to SNG grid injection, which did not provide enough hydrogen production to be
760 sold to mobility distributors for sufficient returns on the high equipment cost.
761 An alternative plant configuration would be to have H₂ mobility as the primary
762 application, with grid injection - preferably pure H₂ if the local grid distribution
763 network allows it - as the secondary application. Indeed, this type of configuration
764 was studied by [20] which also considered it an attractive topology.
765

766 *3.5. Sensitivity Analysis*

767 A sensitivity analysis of the most influential factors for S5 and S8 is done
768 to see their effect on MSP. The electricity price, gas grid availability, electrolyser
769 efficiency and electrolyser and reactor CAPEX are modified by $\pm 20\%$. The data
770 of year 2017 is used due to its better performance in the original analysis.
771 The results are shown in Figure 10.

772 The most influential factor is electrolyser efficiency, which is able to reduce
773 the MSP by 21-24 €/MWh for a minimum of 149.01 €/MWh, due to the



(a) S5 - standard configuration with DA electricity. (b) S8 - CNG mobility with DA electricity.

Figure 10: Tornado charts of S5 and S8 for 2017 showing a $\pm 20\%$ sensitivity analysis on MSP.

774 reduced electricity consumption and thus electricity cost. In contrast, it is
 775 also capable of greatly increasing the MSP if the efficiency were to decrease.
 776 Electricity price is a close second in its impact on MSP, giving the lowest
 777 results in S5 at 153.80 €/MWh and an overall 18-22 €/MWh reduction. The
 778 electrolyser and reactor CAPEX are the next most influential, respectively,
 779 with their impact less than 50% of that done by electricity price. Referencing
 780 Figure 7a showing the total CAPEX portion on scenario LCOM, this relative
 781 impact is to be expected. Grid capacity has extremely little impact on S5
 782 and no impact at all on S8. For S5, this negligible impact is mainly due to
 783 the already high availability of grid injection and variability in times of no
 784 availability: there is almost never long durations in limited grid availability
 785 that would greatly effect production. S5 has 6.5 hours of intermediate H₂
 786 storage that seems to be able to allow production to continue with reduced
 787 grid consumption as per the sensitivity analysis. No impact on S8 is due to
 788 the plant's ability to direct the SNG production to CNG mobility when there

789 is no grid availability.

790 The sensitivity analysis clearly shows the impact of improved electro-
791 lyser efficiency on a PtG plant's profitability. The electrolyser efficiency used
792 is approximately 71% $\left(\frac{5kWh/Nm^3}{3.54kWh/Nm^3 HHV} = 0.71\right)$, meaning efficiency would
793 need to increase to 90% to get similar results as shown. Studies show effi-
794 ciencies of 83% are projected by mid-decade and possibly up to 90% by 2030,
795 suggesting these results could be possible when commercial plants are being
796 deployed [47]. The presented CAPEX reduction is projected to be signifi-
797 cantly surpassed with projections as low as 250 €/kW_{el} by 2030 for PEM
798 electrolyzers [47] and 500 €/kW_{el} for biological reactors [3]. In general, elec-
799 tricity prices are projected to increase as the share of renewables increases in
800 power production, with lower variability in the year due to lower marginal
801 costs [48]. This will mean government support for PtG plants in forms of
802 tax exemptions or other schemes is needed to reduce the primary production
803 cost until CAPEX's or electrolyser efficiency improve.

804 4. Conclusion and Future Work

805 This paper has described a modeling methodology for analysing PtG
806 plants with a special focus on unique local conditions, limitations and op-
807 portunities for the purpose of performing a feasibility analysis for projects.
808 It has shown that these parameters can greatly influence production costs
809 and minimum selling price of product gases, namely synthetic natural gas for
810 the pilot project presented as a case study. Most importantly, the analysis
811 showed that the cost of production is still too high for synthetic natural gas
812 to compete with not only natural gas but biomethane. The current support

813 structure for biomethane in France allows operators to receive a fixed price
814 for production, giving security to their investment. Similar regulation must
815 be put in place for synthetic natural gas, as well as hydrogen grid injection, if
816 France hopes to build up the renewable gas market domestically. These reg-
817 ulations can highlight that power-to-gas plants are not only producing lower
818 emission gases but can also reduce variable renewable energy penetration, if
819 built in strategic locations. In terms of HYCAUNAIS, carbon emissions from
820 the landfill is being reduced as much as possible while maximising methane
821 production, which seeks to benefit all involved.

822 Another positive from power-to-gas facilities is the multiple end-use ap-
823 plications of the product gases. As seen in this analysis, mobility and gas
824 grid injection could both be applied to the plant, provided the additional
825 operational hours and cost don't result in higher levelized costs. Although
826 hydrogen mobility is known to have higher capital costs, this could be out-
827 weighed by the premium price paid at the pump. Primary applications of the
828 plant must be holistically considered to ensure profit maximisation occurs,
829 meaning the main end-use application of the plant should be considered with
830 all local conditions and market values known. A market which was shown
831 to help improve the economics was electricity ancillary services. This added
832 revenue stream could be done without sacrificing production because of an
833 innovative electrolyser design allowing 200% maximum capacity for short
834 durations. If these types of electrolysers were deployed and accepted by
835 regulators for market participation, they can greatly improve power-to-gas
836 business cases.

837 In conclusion, what the analysis has shown is the importance of a qualita-

838 tive survey of a project’s local surroundings. What has been seen in literature
839 to-date are generic analyses of either national power-to-gas potential or plant
840 installation without a full consideration of local limitations or opportunities,
841 such as: natural gas grid availability, all possible gas markets or electricity
842 prices. Individually, these parameters can have profound implications on
843 operational strategy; together they can completely change the plant’s op-
844 erational objective and its feasibility. Meeting climate targets for emission
845 reductions and renewable energy cannot be realized without the help of tech-
846 nologies such as power-to-gas and these technologies cannot be implemented
847 without complex, holistic feasibility analyses.

Funding

This research was supported by the HYCAUNAIS project (agreement number 1882C0096) with financial support provided by the Agency of Ecological Transition in France (ADEME) under the ”Investissements d’Avenir de l’Etat” aid programme, the EIPHI Graduate School (contract number ANR-17-EURE-0002) and the Region Bourgogne Franche-Comté and Bpifrance under ”fond régional d’investissement” (FRI).

References

- [1] European Commission, 2030 climate & energy framework, URL: https://ec.europa.eu/clima/policies/strategies/2030_en#tab-0-0 (2014).
- [2] H. Kondziella, T. Bruckner, Flexibility requirements of renewable energy based electricity systems – a review of research results and

- methodologies, *Renewable and Sustainable Energy Reviews* 53 (2016) 10 – 22. doi:<https://doi.org/10.1016/j.rser.2015.07.199>.
URL <http://www.sciencedirect.com/science/article/pii/S1364032115008643>
- [3] M. Thema, F. Bauer, M. Sterner, Power-to-Gas: Electrolysis and methanation status review, *Renewable and Sustainable Energy Reviews* 112 (2019) 775 – 787. doi:<https://doi.org/10.1016/j.rser.2019.06.030>.
URL <http://www.sciencedirect.com/science/article/pii/S136403211930423X>
- [4] A. Boubenia, A. Hafaifa, A. Kouzou, M. Becherif, Techno economic assessment of hybrid renewable energy systems based on power to hydrogen and methane gas concepts, *Preprints* (2018). doi:10.20944/preprints201809.0023.v1.
- [5] A. Lewandowska-Bernat, U. Desideri, Opportunities of power-to-gas technology in different energy systems architectures, *Applied Energy* 228 (2018) 57–67. doi:<https://doi.org/10.1016/j.apenergy.2018.06.001>.
URL <https://www.sciencedirect.com/science/article/pii/S0306261918308675>
- [6] M. Qadrdan, M. Abeysekera, M. Chaudry, J. Wu, N. Jenkins, Role of power-to-gas in an integrated gas and electricity system in great britain, *International Journal of Hydrogen Energy* 40 (17) (2015) 5763 – 5775. doi:<https://doi.org/10.1016/j.ijhydene.2015.03.004>.
URL <http://www.sciencedirect.com/science/article/pii/S0360319915005418>

- [7] J. Burkhardt, A. Patyk, P. Tanguy, C. Retzke, Hydrogen mobility from wind energy – a life cycle assessment focusing on the fuel supply, *Applied Energy* 181 (2016) 54–64. doi:<https://doi.org/10.1016/j.apenergy.2016.07.104>.
URL <https://www.sciencedirect.com/science/article/pii/S0306261916310492>
- [8] IEA, The Future of Hydrogen – Analysis (Jun. 2019).
URL <https://www.iea.org/reports/the-future-of-hydrogen>
- [9] R. McKenna, Q. Bchini, J. Weinand, J. Michaelis, S. König, W. Köppel, W. Fichtner, The future role of power-to-gas in the energy transition: Regional and local techno-economic analyses in baden-württemberg, *Applied Energy* 212 (2018) 386–400. doi:<https://doi.org/10.1016/j.apenergy.2017.12.017>.
URL <https://www.sciencedirect.com/science/article/pii/S0306261917317312>
- [10] C. Wulf, P. Zapp, A. Schreiber, Review of Power-to-X Demonstration Projects in Europe, *Frontiers in Energy Research* 8 (2020) 191. doi:[10.3389/fenrg.2020.00191](https://doi.org/10.3389/fenrg.2020.00191).
URL <https://www.frontiersin.org/article/10.3389/fenrg.2020.00191>
- [11] M. Götz, J. Lefebvre, F. Mörs, A. McDaniel Koch, F. Graf, S. Bajohr, R. Reimert, T. Kolb, Renewable Power-to-Gas: A technological and economic review, *Renewable Energy* 85 (2016) 1371 – 1390. doi:<https://doi.org/10.1016/j.renene.2015.07.066>.

URL <http://www.sciencedirect.com/science/article/pii/S0960148115301610>

- [12] European Network of Transmission System Operators for Gas, System Development Map, https://entsog.eu/sites/default/files/2021-01/ENTSOG_GIE_SYSDEV_2019-2020_1600x1200_FULL_047.pdf, brussels (2020).
- [13] P. D. Lund, J. Lindgren, J. Mikkola, J. Salpakari, Review of energy system flexibility measures to enable high levels of variable renewable electricity, *Renewable and Sustainable Energy Reviews* 45 (2015) 785 – 807. doi:<https://doi.org/10.1016/j.rser.2015.01.057>.
URL <http://www.sciencedirect.com/science/article/pii/S1364032115000672>
- [14] C. Wulf, J. Linßen, P. Zapp, Review of Power-to-Gas Projects in Europe, *Energy Procedia* 155 (2018) 367 – 378, 12th International Renewable Energy Storage Conference, IRES 2018, 13-15 March 2018, Düsseldorf, Germany. doi:<https://doi.org/10.1016/j.egypro.2018.11.041>.
URL <http://www.sciencedirect.com/science/article/pii/S1876610218309883>
- [15] C. van Leeuwen, A. Zauner, Report on the costs involved with PtG technologies and their potentials across the EU (D8.3), sSTORE&GO Project (2018).
- [16] D. Hissel, Hydrogen economy: myth or reality?, in: *International Smart*

Grid Conference, Paris, France, 2020.

URL <https://hal.archives-ouvertes.fr/hal-02993911>

- [17] J. de Bucy, O. Lacroix, The Potential of Power-to-Gas, Tech. rep., ENEA Consulting, Paris (2016).
- [18] S. McDonagh, R. O’Shea, D. M. Wall, J. Deane, J. D. Murphy, Modelling of a power-to-gas system to predict the levelised cost of energy of an advanced renewable gaseous transport fuel, *Applied Energy* 215 (2018) 444–456. doi:<https://doi.org/10.1016/j.apenergy.2018.02.019>.
URL <https://www.sciencedirect.com/science/article/pii/S0306261918301387>
- [19] C. Breyer, E. Tsupari, V. Tikka, P. Vainikka, Power-to-gas as an emerging profitable business through creating an integrated value chain, *Energy Procedia* 73 (2015) 182 – 189, 9th International Renewable Energy Storage Conference, IRES 2015. doi:<https://doi.org/10.1016/j.egypro.2015.07.668>.
URL <http://www.sciencedirect.com/science/article/pii/S1876610215014368>
- [20] Tractebel, Hincio, Study on early business cases for hydrogen in energy storage and more broadly power to hydrogen applications, Tech. rep., Fuel Cells and Hydrogen 2 Joint Undertaking (2017).
- [21] J. Gorre, F. Ortloff, C. van Leeuwen, Production costs for synthetic methane in 2030 and 2050 of an optimized power-to-gas plant with intermediate hydrogen storage, *Applied Energy* 253 (2019) 113594.

doi:<https://doi.org/10.1016/j.apenergy.2019.113594>.

URL <http://www.sciencedirect.com/science/article/pii/S0306261919312681>

- [22] Agence de la transition écologique, HYCAUNAIS V2, <https://www.ademe.fr/hycaunais-v2> (2019).
- [23] Waga Energy, Technology: WAGABOX, an innovative landfill gas recovery solution, URL: <https://waga-energy.com/en/technology/> (2020).
- [24] GRDF, GRTgaz, SPEGNN, SER, Teréga, Panorama du gaz renouvelable en 2019 (2019).
- [25] IEA, An introduction to biogas and biomethane – Outlook for biogas and biomethane: Prospects for organic growth – Analysis (2020).
URL <https://www.iea.org/reports/outlook-for-biogas-and-biomethane-prospects-for-an-introduction-to-biogas-and-biomethane>
- [26] A. Buttler, H. Spliethoff, Current status of water electrolysis for energy storage, grid balancing and sector coupling via power-to-gas and power-to-liquids: A review, Renewable and Sustainable Energy Reviews 82 (2018) 2440 – 2454. doi:<https://doi.org/10.1016/j.rser.2017.09.003>.
URL <http://www.sciencedirect.com/science/article/pii/S136403211731242X>
- [27] RTE, Règles Services Système Fréquence, <https://www.services-rte.com/files/live/sites/services-rte/files/pdf/>

Service\%20systemes\%20frequence/20181026_Regles_services_systeme_frequence.pdf (2018).

- [28] B. Guinot, F. Montignac, B. Champel, D. Vannucci, Profitability of an electrolysis based hydrogen production plant providing grid balancing services, *International Journal of Hydrogen Energy* 40 (29) (2015) 8778 – 8787. doi:<https://doi.org/10.1016/j.ijhydene.2015.05.033>.
URL <http://www.sciencedirect.com/science/article/pii/S0360319915011775>
- [29] M. Lehner, R. Tichler, H. Steinmuller, M. Koppe, *Power-to-Gas: Technology and Business Models*, Springer, 2014.
- [30] B. Lecker, L. Illi, A. Lemmer, H. Oechsner, Biological hydrogen methanation – a review, *Bioresource Technology* 245 (2017) 1220 – 1228. doi:<https://doi.org/10.1016/j.biortech.2017.08.176>.
URL <http://www.sciencedirect.com/science/article/pii/S0960852417314906>
- [31] J. Gorre, F. Ruoss, H. Karjunen, J. Schaffert, T. Tynjälä, Cost benefits of optimizing hydrogen storage and methanation capacities for Power-to-Gas plants in dynamic operation, *Applied Energy* 257 (2020) 113967. doi:<https://doi.org/10.1016/j.apenergy.2019.113967>.
URL <http://www.sciencedirect.com/science/article/pii/S030626191931654X>
- [32] Electrochaea, *Power-to-Gas via Biological Catalysis (P2G-Biocat) - Final Report*, Tech. rep., Electrochaea, Denmark (2017).

- [33] F. Bauer, T. Persson, C. Hulteberg, D. Tamm, Biogas upgrading – review of commercial technologies, Tech. rep., Swedish Gas Technology Centre, Malmö (2013).
- [34] P. Collet, E. Flottes, A. Favre, L. Raynal, H. Pierre, S. Capela, C. Peregrina, Techno-economic and Life Cycle Assessment of methane production via biogas upgrading and power to gas technology, *Applied Energy* 192 (2017) 282 – 295. doi:<https://doi.org/10.1016/j.apenergy.2016.08.181>.
URL <http://www.sciencedirect.com/science/article/pii/S0306261916312909>
- [35] J. Pépinot, Transport: Les bus à hydrogène de l’Auxerrois mis en service le 1er janvier 2021 pour les voyageurs, URL: <https://www.lyonne.fr/auxerre-89000/actualites/les-bus-a-hydrogene-de-l-auxerrois-mis-en-service-le-1er-janvier-2021-pour-13655307/> (2019).
- [36] M. Smith, J. Gonzales, Costs Associated With Compressed Natural Gas Vehicle Fueling Infrastructure, Tech. rep., National Renewable Energy Lab (9 2014). doi:10.2172/1156975.
- [37] J. André, S. Auray, D. De Wolf, M.-M. Memmah, A. Simonnet, Time development of new hydrogen transmission pipeline networks for France, *International Journal of Hydrogen Energy* 39 (20) (2014) 10323 – 10337. doi:<https://doi.org/10.1016/j.ijhydene.2014.04.190>.
URL <http://www.sciencedirect.com/science/article/pii/S0360319914012804>

- [38] W. Mallon, L. Buit, J. van Wingerden, H. Lemmens, N. H. Eldrup, Costs of CO_2 Transportation Infrastructures, *Energy Procedia* 37 (2013) 2969 – 2980, gHGT-11 Proceedings of the 11th International Conference on Greenhouse Gas Control Technologies, 18-22 November 2012, Kyoto, Japan. doi:<https://doi.org/10.1016/j.egypro.2013.06.183>.
URL <http://www.sciencedirect.com/science/article/pii/S1876610213004268>
- [39] IEA, Countries: France, International Energy Agency, URL: <https://www.iea.org/countries/France> (2020).
- [40] C. van Leeuwen, M. Mulder, Power-to-gas in electricity markets dominated by renewables, *Applied Energy* 232 (2018) 258 – 272. doi:<https://doi.org/10.1016/j.apenergy.2018.09.217>.
URL <http://www.sciencedirect.com/science/article/pii/S0306261918315319>
- [41] RTE, Frequency Ancillary Services Terms and Conditions, https://www.services-rte.com/files/live/sites/services-rte/files/pdf/Service%20systemes%20frequence/SSY_20200530_EN.pdf (2020).
- [42] A. Burke, H. Zhao, Fuel Economy Analysis of Medium/Heavy-duty Trucks – 2015-2050, EVS30 Symposium (10 2017).
- [43] IBNet Tariffs DB, Ville de Strasbourg Water Dept(France), URL: <https://tariffs.ib-net.org/sites/IBNET/ViewTariff?tariffId=18137&countryId=0> (2020).

- [44] RTE, Portail Clients – Réserve contractualisée d'ajustement, URL: https://clients.rte-france.com/lang/fr/visiteurs/vie/reserve_ajustement.jsp (2020).
- [45] EEX, EEX: Natural gas markets, URL: <https://www.powernext.com/natural-gas-trading> (2020).
- [46] M. Lemonde, What is the State of Biogas and Biomethane Market in France?, Biogas World, URL: <https://www.biogasworld.com/news/biogas-biomethane-market-france/> (2020).
- [47] L. Bertuccioli, A. Chan, D. Hart, F. Lehner, B. Madden, E. Standen, Study on development of water electrolysis in the EU, Tech. rep., E4tech Sarl and Element Energy Ltd (2014).
- [48] DNV GL, Imperial College London, NERA Economic Consulting, Integration of Renewable Energy in Europe, https://ec.europa.eu/energy/sites/ener/files/documents/201406_report_renewables_integration_europe.pdf (2014).